Anal. Chem. **2008,** *80,* 9534–9541

Microfluidic Mixers for the Investigation of Rapid Protein Folding Kinetics Using Synchrotron Radiation Circular Dichroism Spectroscopy

Avinash S. Kane,[†,‡] Armin Hoffmann,[§] Peter Baumgärtel,[||] Robert Seckler,[||] Gerd Reichardt,[⊥] David A. Horsley,[‡] Benjamin Schuler,[*,§] and Olgica Bakajin[*,†,‡]

Chemistry, Materials, Life and Earth Sciences Directorate, Lawrence Livermore National Laboratory, 7000 East Avenue, L-233, Livermore, California 94550, University of California, Davis, Davis, California 95817, Biochemisches Institut, Universität Zürich, Winterthurerstrasse 190, 8057 Zürich, Switzerland, Physikalische Biochemie, Universität Potsdam, 14476 Potsdam-Golm, Germany, and Berliner Elektronenspeicherring-Gesellschaft für Synchrotronstrahlung, 12489 Berlin, Germany

We have developed a microfluidic mixer optimized for rapid measurements of protein folding kinetics using synchrotron radiation circular dichroism (SRCD) spectroscopy. The combination of fabrication in fused silica and synchrotron radiation allows measurements at wavelengths below 220 nm, the typical limit of commercial instrumentation. At these wavelengths, the discrimination between the different types of protein secondary structure increases sharply. The device was optimized for rapid mixing at moderate sample consumption by employing a serpentine channel design, resulting in a dead time of less than 200 μs. Here, we discuss the design and fabrication of the mixer and quantify the mixing efficiency using wide-field and confocal epi-fluorescence microscopy. We demonstrate the performance of the device in SRCD measurements of the folding kinetics of cytochrome c, a small, fast-folding protein. Our results show that the combination of SRCD with microfluidic mixing opens new possibilities for investigating rapid conformational changes in biological macromolecules that have previously been inaccessible.

In studies of protein folding kinetics, the folding or unfolding reaction is usually triggered by rapid changes in temperature,[1] pressure,[2] or chemical denaturant concentration.[3] Rapid dilution of chemical denaturants such as guanidinium hydrochloride (GdmCl) or urea is the most commonly used method of starting the folding reaction. The dead time of commercially available stopped-flow mixers that are used to rapidly dilute the denaturant is limited to 0.25 ms under ideal conditions. Typical dead times in commercial instruments using CD spectroscopy are in the range of several milliseconds. Thanks to their rapid mixing time and low sample consumption, microfluidic mixers are being employed increasingly in the studies of folding kinetics. Diffusive mixers with mixing times of 4 μs and femtomole sample consumption have been used to study protein folding using ensemble Förster resonance energy transfer (FRET) spectroscopy.[4] Microfluidic mixers have also been used with single molecule FRET to measure protein folding kinetics and probe the structure of the unfolded state of a protein under folding conditions.[5] Fourier transform-infrared (FT-IR) spectroscopy has been used to probe the α-helix to β-sheet transition in β-lactoglobulin using a diffusive IR mixer.[6] UV fluorescence from tryptophan residues has been used to study the hydrophobic collapse and early folding steps of proteins using a diffusive mixer with a dead time of 20 μs.[7] Small angle X-ray scattering (SAXS) spectroscopy has also been used with mixers to measure the changes in the radius of gyration of cytochrome c.[8,9]

Circular dichroism (CD) is an absorption spectroscopy technique commonly used to identify the secondary structure content of proteins.[10] Protein secondary structures such as α helices and β sheets can be distinguished by their characteristic CD spectra, making CD a powerful method to monitor conformational transitions in biological macromolecules, including protein folding reactions. In contrast to conventional CD sources, synchrotron radiation is a high flux, broadband source of radiation including the far UV (180−250 nm) with high signal-to-noise ratio, permitting measurements below 220 nm, where differences between the CD spectra of the various secondary structure types are often most

* Corresponding authors. E-mail Bakajin1@llnl.gov, phone (925) 422-0931, fax (925) 422-2041 (O.B.). E-mail schuler@bioc.uzh.ch, phone +41 44 635 5535, fax +41 44 635 5907 (B.S.).

† Lawrence Livermore National Laboratory.

‡ University of California, Davis.

§ Universität Zürich.

|| Universität Potsdam.

⊥ Berliner Elektronenspeicherring-Gesellschaft für Synchrotronstrahlung.

(1) Hagen, S. J.; Eaton, W. A. *J. Mol. Biol.* **2000**, *301*, 1019–1027.

(2) Pryse, K. M.; Bruckman, T. G.; Maxfield, B. W.; Elson, E. L. *Biochemistry* **1992**, *31*, 5127–5136.

(3) Chan, C. K.; Hu, Y.; Takahashi, S.; Rousseau, D. L.; Eaton, W. A.; Hofrichter, J. *Proc. Natl. Acad. Sci. U.S.A.* **1997**, *94*, 1779–1784.

(4) Hertzog, D. E.; Ivorra, B.; Mohammadi, B.; Bakajin, O.; Santiago, J. G. *Anal. Chem.* **2006**, *78*, 4299–4306.

(5) Lipman, E. A.; Schuler, B.; Bakajin, O.; Eaton, W. A. *Science* **2003**, *301*, 1233–1235.

(6) Kauffmann, E.; Darnton, N. C.; Austin, R. H.; Batt, C.; Gerwert, K. *Proc. Natl. Acad. Sci. U.S.A.* **2001**, *98*, 6646–6649.

(7) Lapidus, L. J.; Yao, S. H.; McGarrity, K. S.; Hertzog, D. E.; Tubman, E.; Bakajin, O. *Biophys. J.* **2007**, *93*, 218–224.

(8) Pollack, L.; Tate, M. W.; Darnton, N. C.; Knight, J. B.; Gruner, S. M.; Eaton, W. A.; Austin, R. H. *Proc. Natl. Acad. Sci. U.S.A.* **1999**, *96*, 10115–10117.

(9) Akiyama, S.; Takahashi, S.; Kimura, T.; Ishimori, K.; Morishima, I.; Nishikawa, Y.; Fujisawa, T. *Proc. Natl. Acad. Sci. U.S.A.* **2002**, *99*, 1329–1334.

(10) Fasman, G. D. *Circular Dichroism and the Conformational Analysis of Biomolecules*; Plenum Press: New York, 1996.

10.1021/ac801764r CCC: $40.75
Published on Web 11/18/2008

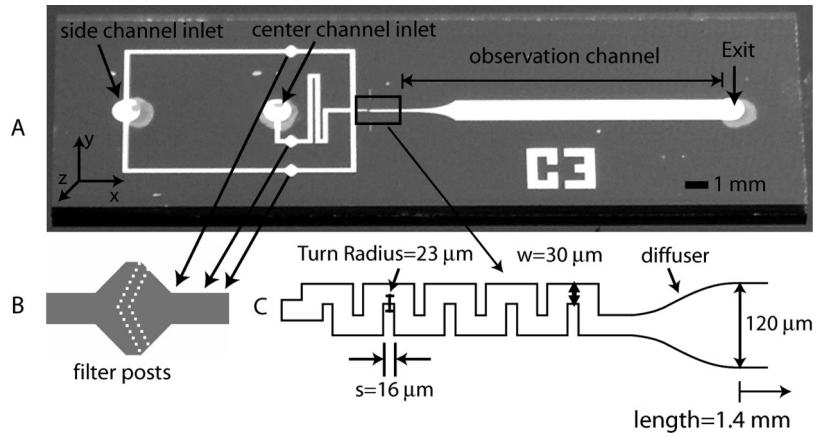

Figure 1. SRCD mixer: (A) photograph of SRCD mixer chip. The aperture is not shown so that details may be easily viewed. (B) Filter posts are designed to minimize clogging of the mixer. (C) Design details of the optimized serpentine mixer showing the channel width, *w*, and turn radius, TR = $^1/_2(w + s)$. The smooth curvature of the diffuser minimizes the creation of any recirculation vortices in the two-section observation channel where kinetics are measured.

pronounced.[11] Akiyama et al.[12] measured kinetics of cytochrome c, a popular model system for rapid protein folding reactions, using a customized conventional CD instrument with a dead time of 0.39 ms and flow rates >20 mL/min.[13] In this study, we describe the development of a new instrument that uses SRCD spectroscopy with a microfluidic mixer, allowing for much lower sample consumption, better dead time, and measurement at 205 nm in the presence of GdmCl. We demonstrate the mixing efficiency of the system using fluorescence microscopy and illustrate its applicability to protein folding in measurements of the microsecond kinetics of secondary structure formation in cytochrome c.

DEVICE DESIGN, MATERIALS, AND FABRICATION

The design of a microfluidic mixer for protein folding is driven by the following figures of merit: dead time, mixing efficiency, and sample consumption. The dead time corresponds to the time difference between the onset of mixing and the first observable point at which experimental data may be measured reliably. The mixing efficiency is a quantitative measure of how well the solutions are mixed. Using SRCD spectroscopy places certain constraints on the design, materials, and fabrication techniques to realize a compatible microfluidic mixer.

Material and Fabrication Constraints. The SRCD mixer needs to be transparent to synchrotron radiation down to 180 nm. Fused silica is a suitable material because it is transparent in the UV and can be micromachined. Since SRCD radiation will be passing directly through the substrate, the etched channel must be sufficiently smooth in order to avoid stray light and to preserve the polarization of the incident light. We determined that deep reactive ion etching (DRIE) provides a suitably smooth channel surface. This technique allows us to create structures with aspect ratios of 3:1 or less.

Mixing Method. A mixer design suitable for our application needs to provide a uniformly mixed solution in the observation region larger than the synchrotron beam. Mixer designs that use turbulence were discarded since this phenomenon occurs only at large Reynolds numbers,[14] implying large channels with high flow rates and excessive sample consumption. Microfluidic devices generally reduce sample consumption but they also exhibit inherently laminar flow, a flow regime which is generally not conducive to fast mixing. Extremely fast mixing times in the laminar flow regime can be achieved using hydrodynamic focusing.[4,15,16] Hydrodynamic focusing has been adapted to wide beams,[5,6] but those designs require high aspect ratio features and multiple etch steps that are difficult to achieve in fused silica. Chaotic advection, where streamlines assume a chaotic trajectory,[17] provides an alternative way to induce mixing. Chaotic advection has been implemented in a variety of microfluidic mixers with periodic perturbations, such as zig-zags,[18] tesla structures,[19] and serpentine shapes.[20−24] We chose to use and optimize the serpentine design because it provides a way to mix solutions in a device whose depth does not change, simplifying the fabrication.

Design and Fabrication of a 2-D Serpentine Mixer for SRCD Spectroscopy. Previously designed serpentine mixers[20–24] are not transparent to synchrotron radiation and do not simultaneously satisfy the requirements of fast dead time (<200 μs) and low sample consumption (<300 μL/min) that we wanted to achieve with our new instrument.

(11) Hoffmann, A.; Kane, A.; Nettels, D.; Hertzog, D. E.; Baumgartel, P.; Lengefeld, J.; Reichardt, G.; Horsley, D. A.; Seckler, R.; Bakajin, O.; Schuler, B. *Proc. Natl. Acad. Sci. U.S.A.* **2007**, *104*, 105–110.
(12) Akiyama, S.; Takahashi, S.; Ishimori, K.; Morishima, I. *Nat. Struct. Biol.* **2000**, *7*, 514–520.
(13) Takahashi, S.; Yeh, S. R.; Das, T. K.; Chan, C. K.; Gottfried, D. S.; Rousseau, D. L. *Nat. Struct. Biol.* **1997**, *4*, 44–50.
(14) Brody, J. P.; Yager, P.; Goldstein, R. E.; Austin, R. H. *Biophys. J.* **1996**, *71*, 3430–3441.
(15) Hertzog, D. E.; Michalet, X.; Jager, M.; Kong, X. X.; Santiago, J. G.; Weiss, S.; Bakajin, O. *Anal. Chem.* **2004**, *76*, 7169–7178.
(16) Yao, S.; Bakajin, O. *Anal. Chem.* **2007**, *79*, 5753–5759.
(17) Ottino, J. M. *The Kinematics of of Mixing, Stretching, Chaos and Transport* Cambridge University Press: Cambridge, U.K., 1989.
(18) Mengeaud, V.; Josserand, J.; Girault, H. H. *Anal. Chem.* **2002**, *74*, 4279–4286.
(19) Hong, C. C.; Choi, J. W.; Ahn, C. H. *Lab Chip* **2004**, *4*, 109–113.
(20) Liu, R. H.; Stremler, M. A.; Sharp, K. V.; Olsen, M. G.; Santiago, J. G.; Adrian, R. J.; Aref, H.; Beebe, D. J. *J. Microelectromech. Syst.* **2000**, *9*, 190–197.
(21) Kim, D. S.; Lee, S. H.; Kwon, T. H.; Ahn, C. H. *Lab Chip* **2005**, *5*, 739–747.
(22) Vijayendran, R. A.; Motsegood, K. M.; Beebe, D. J.; Leckband, D. E. *Langmuir* **2003**, *19*, 1824–1828.
(23) Chamarthy, P.; Wereley, S. T., ASME/IMECE 2004, Anaheim, CA, November 13−14, 2004, Paper No. 2004-61902.
(24) Chen, H.; Meiners, J. C. *Appl. Phys. Lett.* **2004**, *84*, 2193–2195.

In this study, we chose to optimize the design of a 2-D serpentine mixer. In our device, protein solution with high denaturant concentration is injected into the center channel, while the buffer solution that dilutes the denaturant is injected into the side channels (Figure 1A). The two solutions enter the serpentine channel, in which they are mixed in the laminar flow regime by virtue of diffusion and chaotic advection. Secondary or Dean vortices are created in the cross-sectional plane of the channel as the fluid flows through right-angled bends.[25] These vortices arise when centripetal forces are large relative to the viscous forces on the fluid. In pressure-driven flow, the velocity profile is parabolic and the centripetal force is largest at the center of the channel where the maximum velocity occurs, diminishing to zero at the channel walls. As the centripetal force increases in magnitude, an opposing radial pressure gradient is developed. Fluid near the midplane of the channel is driven toward the outer channel wall where it recirculates to the inner channel wall, resulting in Dean vortices. Fluid flow around sharp bends also leads to the creation of corner vortices in the longitudinal plane. At sufficiently high flow rate, the inertia of the fluid does not allow streamlines to "follow" the sharp bends precisely. This effect leads to the creation of a flow-separation region formed by a stagnation point where the streamline velocity is zero. The flow-separation region is not part of the main flow and consists of streamlines recirculating in a region bounded by the inner channel wall and the main flow. At Re > 100, it is the interaction of Dean and corner vortices that stretch, cut, and fold streamlines to produce complete mixing.

After the serpentine channel, the fluid moves through a diffuser (Figure 1C) whose smooth curvature minimizes the creation of any recirculation vortices in the observation channel where kinetics are measured. There are two observation channel sections, which are connected with a logarithmically tapered channel, allowing us to extend the dynamic range of the measurement. Using this design, we can perform both "fast" and "slow" kinetic measurements as the velocity scales with the channel width. The long, wide section also serves to reduce the operating pressure of the device. The variation of the width of the observation channel, although beneficial to increasing the dynamic range of our instrument, also introduced an optical artifact because it changed the amount of collected stray light. Since the stray light affected the SRCD signal, it was necessary to mask off the observation channel with an aperture such that only the CD signal from the inner 100 μm is detected over the entire length of the observation channel (Supporting Information). Filters consisting of arrays of 10 μm × 10 μm posts in each of the side and center channels are designed to minimize clogging of the mixer (Figure 1B).

In this paper, we describe the optimization process of the serpentine mixer geometry in which we considered several design parameters such as the aspect ratio AR (channel depth/width), the number of turns N, and the turn radius TR = $^1/_2(w + s)$ (Figure 1C). The parameter w is the channel width and $(w + s)$ is the spacing between turns. The depth of the channel was dictated by the absorption characteristics of the chemical denaturant, GdmCl, which scales linearly with channel depth.[26a] We determined that channel depths from 10−23 μm would provide an SRCD signal that is strong enough, yet not dominated by GdmCl absorption, so we chose the depth of 15 μm for our study. We explored three different aspect ratios values, AR = 2, 1, and 0.5 corresponding to widths of 7, 15, and 30 μm. Each design also had $N = 5$ or $N = 10$ for the number of serpentine turns. The turn radius TR was fixed at 23 μm in order to be as short as possible to promote chaotic mixing and to minimize the dead time of the mixer. We characterized the extent of mixing in the different designs first using wide field epi-fluorescence, which gives the top-view distribution of mixing while averaging along the depth of the channel (z-direction). We then use confocal microscopy to determine the degree to which solutions are mixed in the z direction.

Serpentine Channel Design for Optimal Mixing Time and Sample Consumption. The design of the mixer was constrained by the dimensions of the synchrotron beam, device burst pressure, and the signal-to-noise ratio in SRCD measurements. The optimization was a tradeoff between dead time and sample consumption. The flow velocity was ultimately limited by the burst pressure, which itself is limited by the mechanical strength of the 175 μm thick fused silica coverslip. The pressure at which bursting occurred was calculated from flow rates to be approximately 260 psi. At this maximum operating pressure, the serpentine designs with AR = 2 and AR = 1 resulted in dead times greater than 200 μs. We verified that the design with AR = 0.5 and $N = 5$ turns had the best performance by experimentally characterizing the mixing efficiency (see the Results and Discussion). The calculated mixing time, at a point immediately after the diffuser, was t_{mix} = 140 μs at a total flow rate of 250 μL/min, corresponding to an operating pressure of 230 psi. At this flow rate, it takes about 8 μs for the fluids to traverse the beam (calculated as the ratio of the synchrotron beam width (20 μm) to the average velocity of 2.36 m/s in the narrow part of the observation channel), indicating that the mixing time ($\gg$8 μs) determines the uncertainty in time for our measurement. A deeper channel with lower impedance would allow for higher flow velocity at the maximum operating pressure, implying a shorter mixing time but at the expense of increased sample consumption and higher GdmCl absorption. A thicker coverslip extends the operating pressure of the mixer but is incompatible with the high numerical aperture, short working distance objectives used in confocal microscopy.

METHODS

Mixer Fabrication Process. Mixers are fabricated in 500 μm thick fused silica wafers (Corning 7980, 0F grade) using a deep reactive ion etching process with nearly vertical sidewalls. In order to bulk micromachine the fused silica substrate, a suitable masking layer must be deposited to accommodate the dry etching process. A 2.0 μm thick undoped polysilicon mask is grown in a low pressure chemical vapor deposition (LPCVD) furnace at a temperature of 625 °C on the fused silica substrate. The process gas is SiH_4 at a flow rate of 250 sccm (standard cubic centimeter per minute), and the chamber pressure is 500 mTorr. A typical deposition rate is 75 Å per min. The first mask containing the mixer pattern is used to perform photolithography on the substrate. The polysilicon layer is etched down to the fused silica

(25) Vanka, S. P.; Luo, G.; Winkler, C. M. *AIChE J.* **2004**, *50*, 2359–2368.

(26) (a) Johnson, W. C. in *Circular Dichroism and the Conformational Analysis of Biomolecules*; Fasman, G. D., Ed.; Plenum Press: New York, 1996; pp 635−652. (b) Sutherland, J. C. in *Circular Dichroism and the Conformational Analysis of Biomolecules*; Fasman, G. D., Ed.; Plenum Press: New York, 1996; pp 599−633.

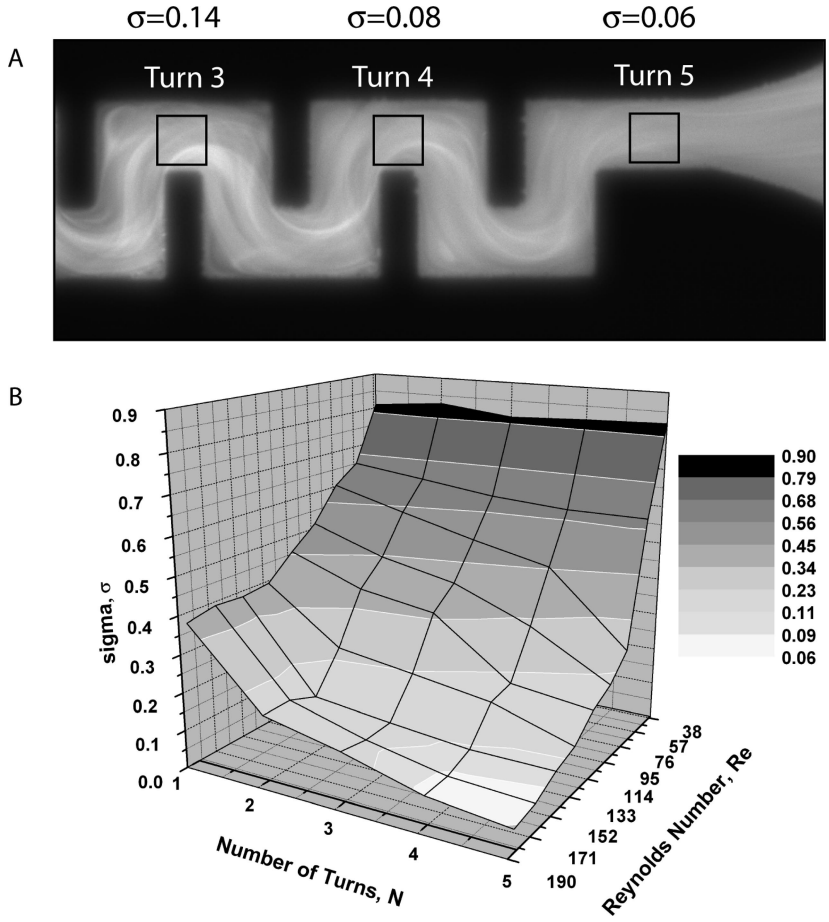

Figure 2. (A) Wide field epi-fluorescence image of a mixer with AR = 0.5 at a total flow rate of 250 μL/min (Re = 185). Pixel data is taken from the 25 μm × 25 μm region of interest (ROI) inside the drawn black square at turns 3, 4, and 5. The calculated σ values are $\sigma = 0.14$ at turn 3, $\sigma = 0.08$ at turn 4, and $\sigma = 0.06$ at turn 5. (B) Surface plot of σ as a function of the number of turns, *N*, and the Reynolds number, Re. This plot allows the designer to determine the number of turns and Reynolds number required for a particular value of σ. σ decreases with both the Reynolds number and number of turns.

using a Surface Technology Systems (STS, Newport, U.K.) deep reactive ion etcher (DRIE). The fused silica substrate is then etched using an STS Advanced Oxide Etcher (AOE) to a depth of 15 μm. The AOE provides an etch selectivity of approximately 17:1 between polysilicon and fused silica. The polysilicon mask is then removed with a XeF_2 etcher. Inlet holes are implemented though the use of micro-sandblasting. Sealing of microfluidic mixers is accomplished by direct fusion wafer bonding to another 175 μm thick fused silica substrate. Both the etched and cover substrates are thoroughly cleaned using piranha solution (sulfuric acid + hydrogen peroxide) and a reverse RCA cleaning procedure. Following the piranha etch, the substrates are cleaned for 20 min in 5:1:1 $H_2O/NH_4OH/H_2O_2$ solution at a temperature of 72 °C. After drying, the substrates are joined together and then annealed at 1100 °C. The aluminum aperture is next implemented by performing photolithography on the bonded wafer stack. A 150 nm thick aluminum aperture with a 100 μm gap has been implemented through a standard liftoff process. The aperture straddles the centerline of the observation channel, leaving a gap of 100 μm to allow for acceptable tolerances during photolithographic alignment to the 120 μm observation channel.

Sample Preparation. Oxidized horse heart cytochrome c (cyt c, from Sigma Aldrich Co., St. Louis, MO) was diluted in unfolding buffer (4 M GdmCl, 100 mM sodium phosphate, pH 7) to a final concentration of 50 g/L. For the reference measurements, this solution was diluted 4-fold either with unfolding or refolding buffer (100 mM sodium phosphate, pH 7). All solutions were filtered (0.22 μm). The reference measurements were performed at the same total flow rate as in the mixing measurements, 250 μL per min. For all measurements, buffer spectra where taken under exactly the same conditions and subtracted from the protein spectra.

Experimental Setup: SRCD. The experimental setup of our synchrotron CD measurements was similar to the one described by Sutherland.[26b] As a synchrotron light source we used the undulator beam line U125/2-10m NIM at BESSY II.[27] A LiF window (Korth Kristalle GmbH, Altenholz, Germany) separates the ultrahigh vacuum of the beam line from the experimental chamber under atmospheric pressure. As the pressure difference introduces stress birefringence in the LiF window, a MgF_2 Rochon polarizer (B. Halle Nachfl. GmbH, Berlin, Germany) followed in the optical path to ensure linear polarization. A photoelastic modulator (PEM) (Hinds Instruments, Hillsboro; model I/CF50) for converting the linearly polarized light into circularly polarized light was used. A Suprasil-lens (B. Halle Nachfl. GmbH, Berlin,

(27) Reichardt, G.; Bahrdt, J.; Schmidt, J. S.; Gudat, W.; Ehresmann, A.; Muller-Albrecht, R.; Molter, H.; Schmoranzer, H.; Martins, M.; Schwentner, N.; Sasaki, S. *Nucl. Instrum. Methods Phys. Res., Sect. A* **2001**, *467*, 462–465.

Germany) with a focal length of 10 mm (at $\lambda = 200$ nm) focused the beam to a spot size of 20 (±2) μm horizontally and 60 (±5) μm vertically (full width at half-maximum) parallel and perpendicular to the direction of sample flow, respectively. Three motorized translation stages (Physik Instrumente, Karlsruhe, Germany; model M-111.1) allowed movement of the mounted microfluidic device and enabled precise positioning of the focused synchrotron beam within the observation channel. The flow rates of the sample were controlled by precision syringe pumps as described in the next section. The transmitted light was detected with a low noise, solar blind channel photomultiplier (Perkin-Elmer, Waltham, MA, model CPM 1321). The photon flux at the sample position at 204 nm was about 5×10^{10} photons/s and at 220 nm about 5×10^{11} photons/s at a bandwidth of 0.3 nm. The absolute CD sensitivity of the setup was calibrated with the calibration standard (+)-10-camphorsulfonic acid (CSA).[28]

MEASUREMENTS OF MIXING EFFICIENCY

Wide Field Epi-Fluorescent Microscopy and Image Analysis. Mixing was first observed through a wide field epi-fluorescent microscope. Mixing is observed as a function of flow rate by measuring the fluorescence intensity of 10 μM fluorescein mixed with 100 mM phosphate buffered saline (PBS). The mixer chip was mounted on an acrylic holder and then placed on the stage of a Nikon TE2000-U inverted microscope. A mercury lamp was used for illumination. Images were recorded with a Coolsnap FX CCD camera (Roper Scientific, Inc., Tuscon, AZ) through a 20× objective, NA = 0.40 with resolution 0.25 μm/pixel. The center and side channels were each connected to separate PHD 2000 syringe pumps (Harvard Apparatus) through the use of Teflon tubing and Upchurch fittings. Hamilton gastight syringes of 7.28 and 10.3 mm diameters were used for the center and side channels, respectively. The center channel contained the fluorescein solution and the side channel contained the PBS solution. The two solutions were mixed in the ratio 1:4.

In order to quantify the mixing process, we define σ as a measure of inhomogeneity of the solution. Its definition is based on the standard deviation of the pixel intensity and the average intensity in a given region of interest (ROI) in the serpentine channel:

$$\sigma = \frac{\sqrt{\frac{1}{n}\sum_{i=1}^{n}(I_i - \langle I \rangle)^2}}{\langle I \rangle} \quad (1)$$

where I_i is the background-corrected value of the ith pixel, $\langle I \rangle$ is the average value of the background corrected intensity, and n is the total number of pixels in the ROI. In our analysis of wide field epi-fluorescence images, a ROI of 100 × 100 pixels is chosen, corresponding to physical dimensions of 25 μm × 25 μm. In the absence of instrumental noise, the distribution of intensities in a completely mixed solution should have a σ value of 0. In reality, noise introduces a variation in fluorescence intensity even for completely mixed solutions and results in a nonzero σ.[29] In order to measure this noise value, we calculated σ for the image of a homogeneous fluorescein solution in the channel (i.e., premixed fluorescein in PBS buffer in the volume ratio 1:4) and obtained a value of $\sigma = 0.04$. Mixing images were recorded over a range of Reynolds numbers, $37 \leq \mathrm{Re} \leq 185$, with the corresponding σ values calculated at each of the 5 turns.

Confocal Microscopy and Image Analysis. Mixing was also observed with a confocal microscope. A CW argon ion laser (Coherent, Inc., Santa Clara, CA) provides excitation at 488 nm through an inverted microscope (Nikon Eclipse TE300) with a 60×, 0.8 NA objective. The fluorescent signal was collected with the same objective and passed through a dichroic mirror and a 50 μm pinhole to an avalanche photodiode (APD, Perkin-Elmer Optoelectronics, Fremont, CA). A three-axis piezoelectric stage (Physik Instrumente, Germany) with nanometer resolution was used to scan confocal images. The stage was controlled with custom software developed in LabView (National Instruments, Austin, TX). The integration time per pixel was 10 ms. Scans were performed at the fifth turn of the serpentine channel and were in the cross-sectional plane of the channel (*YZ* plane). Each scan was 50 μm wide (transverse, *Y*-direction) and 20 μm deep (*Z*-direction). The resolution was 0.25 μm/pixel in the *Y*-direction and 0.20 μm/pixel in the *Z*-direction. Mixing experiments at the viscosity of water were performed with 10 μM fluorescein solution and 100 mM PBS under the same conditions as the previous epi-fluorescent experiments. Mixing experiments at higher viscosity were performed with 10% w/w glycerol in 10 μM fluorescein solution and 100 mM PBS buffer. We adjusted the viscosity to match the viscosity of 4.0 M GdmCl solution used in the protein folding kinetics experiments (30% higher than water at 20 °C). The mixing efficiency for confocal measurements is defined the same way as for the wide-field epi-fluorescence experiments. The ROI is chosen to be 40 × 80 pixels (8 μm × 20 μm) to remove variations in the fluorescence intensity from optical effects at the channel walls. A noise value of $\sigma = 0.07$ was calculated for both aqueous and viscous premixed images.

RESULTS AND DISCUSSION

Quantification of Mixing Using Wide-Field Epi-Fluorescent Imaging. The mixing efficiency of the optimized serpentine mixer was first studied as a function of the number of turns and Reynolds number using wide-field epi-fluorescence microscopy. We compared two designs with AR = 0.5, one with $N = 5$ turns and the other with $N = 10$. An optimal mixing efficiency that corresponds to $\sigma = 0.06$ was achieved with both designs but at different Reynolds numbers. For the 10 turn mixer, optimal mixing was achieved at Re = 111, while for the mixer with 5 turns, it was achieved at Re = 185. Figure 2A shows the progressive improvement in mixing efficiency with increasing number of turns at Re=185. The overall mixing performance is summarized by the surface plot in Figure 2B, showing the σ value as a function of the number of turns, *N*, and Reynolds number, Re. This plot allows the designer to determine the parameters required for a particular value of mixing efficiency. As expected, the mixing efficiency improves (σ decreases) with both Reynolds number and *N*.

Quantification of Mixing Using Confocal Imaging. Confocal imaging was performed on the optimized five-turn mixer design to additionally investigate the degree of mixing in the *z*-direction. In addition to measuring mixing for solutions with viscosity equal

(28) Chen, G. C.; Yang, J. T. *Anal. Lett.* **1977**, *10*, 1195–1207.
(29) Floyd-Smith, T. M.; Golden, J. P.; Howell, P. B.; Ligler, F. S. *Microfluid. Nanofluid.* **2006**, *2*, 180–183.

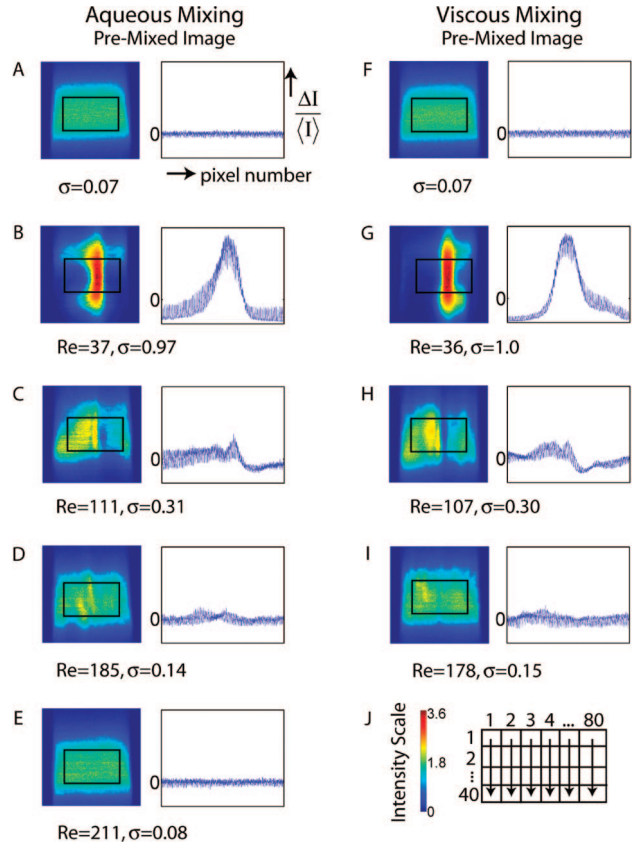

Figure 3. A comparison of confocal images obtained for aqueous and viscous mixing experiments at various Reynolds numbers. The first column corresponds to the aqueous case (A−E) while the second corresponds to the viscous case (F−I). Each panel shows a confocal image with the 40 pixel × 80 pixel (8 μm × 20 μm) ROI indicated by the rectangle. In order to visualize σ and the variation in the pixel intensity across the ROI, the difference between intensity for a given pixel and the average intensity, normalized by the average intensity, is plotted for every pixel. The pixel number value is raster-scanned column by column as illustrated in panel J to cover the entire ROI. The percent difference scale on the *y*-axis varies from −100% to 300%, and the pixel number on the *x*-axis ranges from 1 to 3200 for all plots. The premixed images are shown in panels A and F along with the following flow rates (B,G) 50, (C,H) 150, (D,I) 250, and (E) 285 μL/min. The color map (J) indicates fluorescence intensity.

to that of water (aqueous), we also performed measurements on more viscous solutions to mimic the effects of denaturant GdmCl used in protein folding experiments. Figure 3 summarizes the results of confocal imaging at various total flow rates and corresponding Reynolds numbers for both aqueous and viscous cases. The best mixing, which corresponds to $\sigma = 0.08$ (note that $\sigma = 0.07$ is the measured noise level using this imaging method) was achieved at 285 μL/min, Re = 211. The highest mixing efficiency that was measured in the viscous experiment was $\sigma = 0.15$ at a total flow rate of 250 μL/min (Re = 178). Attempts to perform the viscous mixing experiments at higher flow rates caused bursting of the chips due to excessive back-pressure. Figure 4 shows a comparison of measurements by wide-field and confocal epi-fluorescence microscopy. Mixing efficiencies measured over a range of Reynolds number $36 \leq Re \leq 185$ show that wide field epi-fluorescence results in better σ values. This observation is consistent with the fact that in wide-field measurements, the pixel intensity values are averaged along the depth of

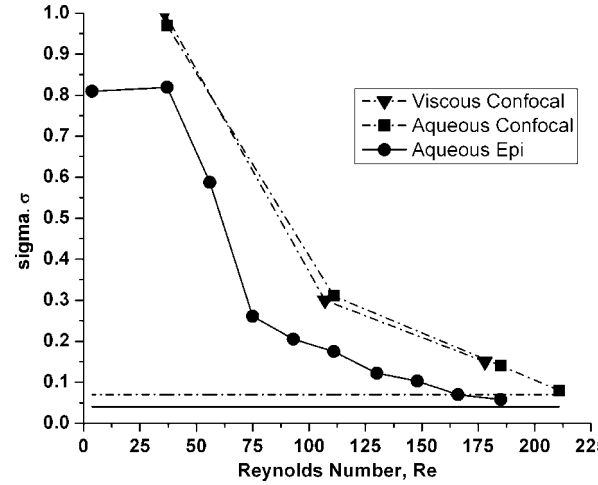

Figure 4. A plot of σ, as a function of Reynolds number, Re, for confocal measurements in the aqueous (■) and viscous case (▼) as well as wide-field epi-fluorescent imaging in the aqueous case (●). Horizontal lines correspond to the values of σ obtained for premixed solutions from confocal (dashed line) and wide field epi-fluorescence (full line) images, showing that the mixer approaches perfect mixing at large Re.

the channel (*z*-direction). However, at flow rates ≥250 μL/min, using the two imaging methods we measure similar differences between the premixed and the mixed σ values indicating that both imaging methods can be used to measure mixing efficiency. Wide-field epi-fluorescence is particularly useful for parametric studies since it is less labor intensive and time-consuming than scanning confocal microscopy. Figure 4 also shows that the 30% increase in viscosity of one of the solutions does not considerably reduce the mixing efficiency. However, increased viscosity does increase the pressure drop in the device and dictates a lower maximum operating flow rate.

SRCD Spectroscopy of Rapid Protein Folding Kinetics. To demonstrate the performance of the optimized mixer design in monitoring rapid protein folding reactions, we performed SRCD spectroscopy measurements at BESSY II on the small protein cytochrome c. The refolding reaction was initiated by a 4-fold dilution of cyt c in 4 M GdmCl with refolding buffer to a final GdmCl concentration of 0.8 M. The measurement was performed at a total flow rate of 250 μL/min (Re = 178), corresponding to $\sigma = 0.15$ mixing efficiency measured using the confocal setup.

At the first measurement position in the channel, corresponding to $t_{dead} = 180$ μs after mixing, spectra were taken both for the refolding reaction and under equilibrium start (4 M GdmCl) and end (0.8 M GdmCl) conditions (Figure 5B). The reference spectra at 4 and 0.8 M are typical of an unfolded protein and a folded α-helical protein, respectively.[10] A linear combination of both reference spectra shows that the spectrum acquired 180 μs after the start of refolding corresponds to about 28 ± 6% folded signal. Note that the reference with 4 M GdmCl can be measured down to 205 nm, significantly lower than accessible in conventional stopped-flow CD instrumentation.

We also measured the kinetic progress curve of the refolding reaction at 220 nm along the entire observation channel (up to 30 ms, Figure 5A). The refolding trace was fit with a single exponential with a refolding rate of 190 ± 25 s^{-1}. The accessible time window covers 44 ± 2% of the total signal change. A change

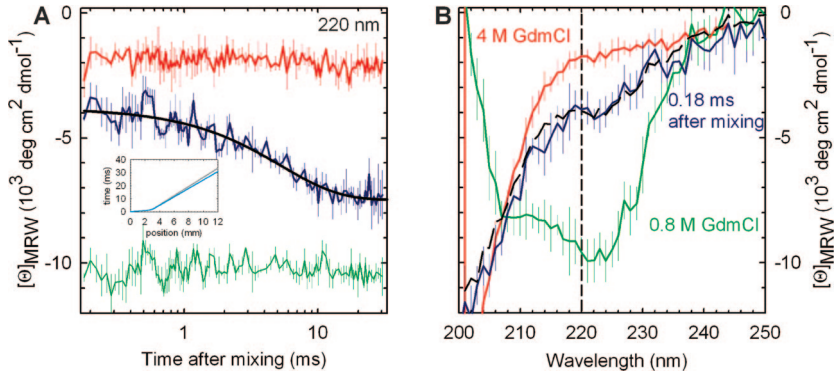

Figure 5. Synchrotron radiation circular dichroism measurements of cyt c in the mixing device. Kinetic measurements under refolding conditions are show in blue, measurements under equilibrium conditions representing the start (4 M GdmCl) and end conditions (0.8 M GdmCl) are shown in red and green, respectively. Error bars show the standard deviation calculated from two kinetic traces (A) or three spectra (B). (A) Refolding kinetics measured at 220 nm and single exponential fit to the data (black). (B) CD spectra measured at 0.18 ms after mixing and linear combination of 28% native and 72% unfolded spectra (black dashed line) The inset in part a shows the time versus position conversion function in the mixer using the average flow rate over the entire channel (gray) and the average flow rate over the calculated spot size (blue), demonstrating that neglecting the shape of the flow profile does not significantly influence the calculation of the time after mixing.

of 22 ± 2% already occurred in the dead time of our instrument, and 33 ± 2% of the signal is still missing after 30 ms. As expected, the reference spectra under equilibrium conditions are invariant along the channel and show the CD signal characteristic of folded and unfolded protein, respectively.

The fast refolding kinetics of cyt c have been studied in great detail,[30−33] which makes cyt c an ideal reference for rapid mixing experiments. The refolding mechanism of cyt c has been shown to exhibit at least three phases: a fast collapse with a rate constant of about 20 ms^{-1} (ref 33) and a change of the CD signal amplitude at 222 nm of about 25%, an increase of the helical secondary structure of about 49% during a second phase with a rate constant of 300 s^{-1}, and a third phase leading to the folded state with a rate constant of about 13 s^{-1}. [12] In the time range accessible with our current instrument design, we can resolve the rate constant of the largest amplitude phase. The good agreement with the rate of the major phase and the amplitudes observed by Akiyama et al.[12] thus provide a stringent test of the capabilities of SRCD in combination with microfluidic devices. The agreement also demonstrates that the effects of flow profile in *y* and *z* on the measurement of cytochrome c kinetics at this flow rate are small, as supported by the confocal image from Figure 3I and the very small difference in the time after mixing when averaged over the spotsize vs over the whole channel (inset in Figure 5A). The profile in *y* and *z* in the observation region somewhat decreases the time resolution and is captured in the overall uncertainty of our measurement. In summary, the novel combination of SRCD spectroscopy with microfluidic mixing devices opens new opportunities to probe structural changes in biomolecules on previously inaccessible time scales and wavelength ranges. Our device provides an unprecedented dead time for CD experiments in the presence of buffers with high absorption (GdmCl) and clearly demonstrates the potential of the method.

Future improvements in the approach described here are to be expected, especially with the advent of dedicated SRCD beam lines, which are under construction or already in operation at several synchrotrons.[34,35] Higher photon flux will improve the signal-to-noise ratio, accelerate data acquisition, thus reduce sample consumption, enable the use of lower protein concentrations, and possibly allow a further extension of the accessible wavelength range and the use of deeper channels. Of particular importance for the combination with microfluidic mixing is the brilliance of synchrotron sources, allowing the efficient focusing of light into microstructures. Future developments in beam quality and microfabrication are thus expected to enable further improvements in dead time and time resolution. An SRCD beamline optimized specifically for use with microfluidic devices is currently under construction at BESSY. The work presented here presents guidelines for optimizing the mixer geometry for the specific requirements of the synchrotron radiation source and provides an important step toward making kinetic SRCD spectroscopy more broadly available.

ACKNOWLEDGMENT

We thank Shuhuai Yao and David Hertzog for technical assistance and discussions. This work has been supported by the Human Frontier Science Program (A.S.K., O.B., A.H., B.S.), the Schweizerische Nationalfonds (B.S.), and the Deutsche Forschungsgemeinschaft (R.S.). The work of O.B. and A.S.K. was performed at Lawrence Livermore National Laboratory with the support of the LDRD program. Lawrence Livermore National Laboratory is operated by Lawrence Livermore National Security, LLC, for the U.S. Department of Energy, National Nuclear Security Administration under Contract DE-AC52-07NA27344 and partially supported by funding from the Center for Biophotonics, an NSF Science and Technology Center, managed by the University of California, Davis, under

(30) Chan, C. K.; Hu, Y.; Takahashi, S.; Rousseau, D. L.; Eaton, W. A.; Hofrichter, J. *Proc. Natl. Acad. Sci. U.S.A.* **1997**, *94*, 1779–1784.
(31) Winkler, J. R. *Curr. Opin. Chem. Biol.* **2004**, *8*, 169–174.
(32) Elove, G. A.; Chaffotte, A. F.; Roder, H.; Goldberg, M. E. *Biochemistry* **1992**, *31*, 6876–6883.
(33) Shastry, M. C.; Roder, H. *Nat. Struct. Biol.* **1998**, *5*, 385–392.
(34) Miles, A. J.; Hoffmann, S. V.; Tao, Y.; Janes, R. W.; Wallace, B. A. *Spectrosc: Int. J.* **2007**, *21*, 245–255.
(35) Miron, S.; Refregiers, M.; Gilles, A. M.; Maurizot, J. C. *Biochim. Biophys. Acta* **2005**, *1724*, 425–431.

Cooperative Agreement No. PHY 0120999. A.S.K. was also supported by the SEGRF Program at LLNL and his trips to Germany were supported by travel awards through U.S. National Science Foundation I2CAM International Materials Institute Award, Grant DMR-0645461. R.S., P.B., and the SRCD station at BESSY are supported by the German Federal Ministry of Education and Research (BMBF), Contract 05 KS4IP1/2.

SUPPORTING INFORMATION AVAILABLE

Additional information as noted in text. This material is available free of charge via the Internet at http://pubs.acs.org.

Received for review August 21, 2008. Accepted October 8, 2008.

AC801764R

Supplementary Information

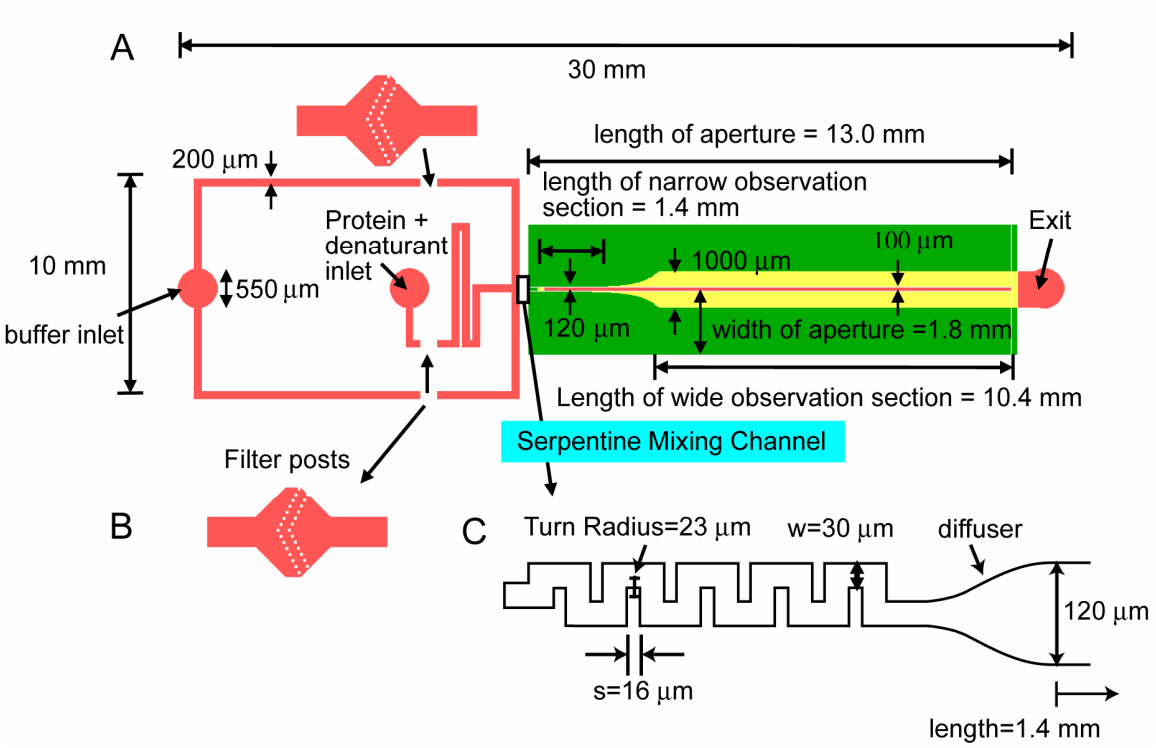

Supplementary Figure 1: SRCD Mixer. (A) Schematic diagram showing design details of the optimized 5-turn mixer. The topside aperture is shown in (green) straddling the two-section observation channel with a gap of 100 µm. The first section of the observation channel is 120 µm wide and is 1.4 mm long. The second section is 1000 µm wide and 10.4 mm long. (B) Filter posts consisting of arrays of 10 µm X 10 µm pillars in each of the buffer and protein channels are designed to minimize clogging of the mixer. (C) Design details of the optimized serpentine channel showing the channel width, w, and turn radius TR=1/2(w+s). The smooth curvature of the diffuser minimizes the creation of any recirculation vortices in the two-section observation channel where kinetics are measured.

Calculation of the time after mixing from the position in the observation channel

The time t after mixing at a point x was calculated as

$$t(x) = \frac{V(x)}{\dot{V}} + t_{dead}\,, \tag{S1}$$

where $V(x)$ is the volume between the starting point of the observation region and $x, \dot{V}$ is the total flow rate, and t_{dead} is the deadtime of the mixer at the chosen flow rate.

We used a laminar flow profile (1) to calculate the position-dependent flow velocity v as

$$v(y,z) = A \times \sum_{i=1,3,5,\ldots}^{\infty} (-1)^{(i-1)/2} \times \left(1 - \frac{\cosh\left(i\pi z/2a\right)}{\cosh\left(i\pi b/2a\right)}\right) \times \frac{\cos\left(i\pi y/2a\right)}{i^3}, \tag{S2}$$

where a denotes the width and b the depth of the channel. y and z originate from the center of the channel cross section and indicate the coordinates in the direction of channel width and depth, respectively. The prefactor A is adjusted to get the known flow rate when v is integrated over the whole channel. Note, however, that in the ratio of the average flowrate in the synchrotron beam v_{beam} and in the whole channel $v_{channel}$, A cancels, and for our geometry we obtain:

$$\frac{v_{beam}}{v_{channel}} = \frac{\int_{y=0}^{30}\int_{z=0}^{7} v(y,z)\,dy\,dz}{\int_{y=0}^{60}\int_{z=0}^{7} v(y,z)\,dy\,dz} = 1.081\,. \tag{S3}$$

Using this approach, we find a total flow rate of 270 uL/min in the part of the cross section where the beam passes over the channel. Over the range of observation positions, the time versus position conversion function is affected only slightly compared to the average over the entire channel, as shown in the inset to figure 5.

(1) White, F. M. *Viscous Fluid Flow* **1991** (New York: McGraw-Hill)